A simple state-of-the-art spectrometer for student labs: Cost-efficient, instructive, and widely applicable

Andreas Eggenberger

; Tomasz Smolenski; Martin Kroner



Am. J. Phys. 92, 146–153 (2024) https://doi.org/10.1119/5.0164044





CrossMark

01 February 2024 17:11:46







INSTRUCTIONAL LABORATORIES AND DEMONSTRATIONS

John Essick, Editor

Department of Physics, Reed College, Portland, OR 97202

Articles in this section deal with new ideas and techniques for instructional laboratory experiments, for demonstrations, and for equipment that can be used in either. Although these facets of instruction also appear in regular articles, this section is for papers that primarily focus on equipment, materials, and how they are used in instruction. Manuscripts should be submitted using the web-based system that can be accessed via the American Journal of Physics home page, ajp.aapt.org, and will be forwarded to the IL&D editor for consideration.

A simple state-of-the-art spectrometer for student labs: Cost-efficient, instructive, and widely applicable

Andreas Eggenberger, a) Tomasz Smolenski, and Martin Kroner (b) Department of Physics, ETH Zuerich, CH-8093 Zürich, Switzerland

(Received 20 June 2023; accepted 9 October 2023)

We present a simple, cost-effective, yet instructive spectrometer for use in undergraduate instructional laboratory courses. Deliberate design choices are made to enhance the learning experience provided by the setup, where every component is accessible to students, allowing them to fully understand the function of each individual item. The result is a state-of-the-art spectrometer, built from commercially available components, which balances pedagogical simplicity with the potential for a wide range of applications. Our setup prepares students for future spectroscopy work in research labs. Furthermore, data-taking by means of a CCD camera and the subsequent analysis teach students fundamental computational skills. Within one image, the spectrometer can cover a spectral range of 40 nm and its spectral resolution is about 0.1 nm, limited by the imaging optics. Systematic uncertainties arising from mechanical play of the grating's rotation stage limit the reproducibility of the setup to 0.65 nm. While these parameters can be improved, we decided to maintain the pedagogical and straightforward nature of the presented setup, as any increase in cost or complexity would undermine its educational benefits. Using the spectrometer in an undergraduate instructional laboratory makes possible a variety of valuable experiments, such as calibration measurements, investigation of different types of uncertainties and measurements errors, and historically important measurements (e.g., the Balmer series or solar spectrum). We are convinced that the presented spectrometer will greatly benefit the learning experience of students for many years to come. © 2024 Author(s). All article content, except where otherwise noted, is licensed under a Creative Commons Attribution (CC BY) license (http://creativecommons.org/licenses/by/4.0/). https://doi.org/10.1119/5.0164044

I. INTRODUCTION

Optical spectroscopy plays an important role in science and technology: observing atomic spectral lines and the blackbody radiation spectrum was decisive in the development of quantum mechanics and progressing our understanding of nature. Still, spectroscopy remains an indispensable tool in modern research ranging from physics and astronomy to chemistry and biology. Furthermore, optical spectroscopy is an essential technological tool widely used in applications such as meteorology, materials analysis, and telecommunication.

Consequently, undergraduate physics students encounter optical spectra very early on in their courses. It is essential to augment this theoretical understanding with hands-on experience in laboratory experiments. This lab experience allows students to consolidate their understanding of the physics of diffraction, to strengthen their grasp of the physics of resonances and energy levels, and to forge links between classical and quantum mechanics. The combination of these three features makes spectroscopy experiments a valuable and essential tool in practical physics education.

The traditional type of spectrometer that students might encounter in a lab course is a prism or grating spectrometer, mounted on a rotating stage. Two optical tubes, a collimator and a telescope, collimate the light of a vapor lamp, guiding it through the optical element toward the observer. Depending on the angle between the two tubes and the angular position of the prism or grating, a certain wavelength is projected toward the observer.

Such prism spectrometers have moderate resolution and, because observation is done by eye, they provide qualitative rather than quantitative results. Therefore, while these spectrometers serve instructional purposes, they have a limited field of application. Although these instruments are suitable for demonstration purposes, working on such spectrometers does not prepare students for their future work in research



laboratories. Finally, these setups are usually expensive to purchase, have limited customization options, or require extensive use of a workshop to manufacture.

Another class of spectrometers encountered in educational physics labs are ready-to-use spectrometers, which can be bought from various companies, e.g., from Thorlabs. These products are designed to be plug-and-play devices, making them highly convenient for everyday use in research laboratories. However, they do not possess the capability to effectively teach students the fundamental principles of spectroscopy. In this work, we explicitly do not aim to compete with these plug-and-play devices concerning cost and resolution, as we believe they serve a different purpose. Our focus is to provide a learning experience that imparts a deep understanding of spectroscopic concepts.

Therefore, we present here a spectrometer that can be easily built with commercially available components at a reasonable cost without the need for a workshop (for a complete list of the components, please refer to Table I in Appendix C). Our instrument is highly versatile and allows one to conduct many fundamental and advanced experiments within the scope of student labs. Being a state-of-the-art setup, it has high resolution and allows for very precise measurements, which increases the motivation of students. Nevertheless, the goal is not to achieve the highest possible resolution or detection efficiency, but rather to provide a simple and cost-effective setup that can be easily understood by undergraduate physics students. It is even possible to have the students assemble the spectrometer themselves, as it consists of only five main items and can be set up in short time. Hence, the presented spectrometer is optimized for maximal pedagogical value.

II. DESCRIPTION OF THE SPECTROMETER

The setup that we developed follows the design of a symmetric Czerny–Turner grating spectrometer. ^{2,3} We use off-center parabolic mirrors in a symmetric configuration. ^{4,5} In this way, we can reduce aberrations to a negligible level for educational purposes. A list of the components is included in Appendix C.

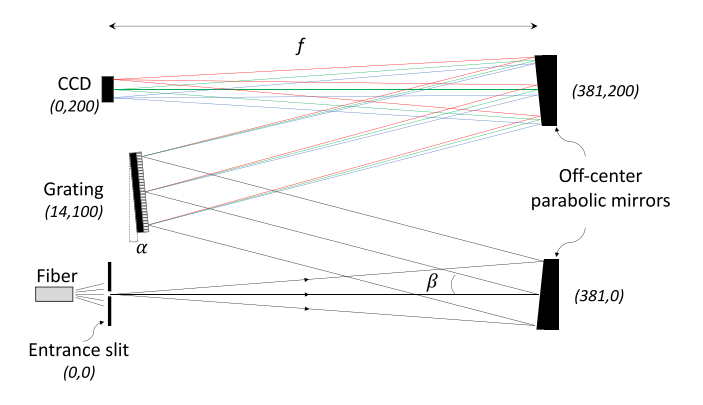


Fig. 1. (Color online) Schematic sketch of the Czerny–Turner spectrometer design. The spectrometer features an entrance slit, an off-center parabolic mirror that collimates the light, a ruled reflective grating that disperses the light, and a second off-center parabolic mirror that focuses the light on the CCD camera, which is then used to record the measured spectrum. In brackets, the position of every element relative to the entrance slit is indicated in millimeters. The wavelength of lines visible in the spectrum is determined by the angle α of the grating that can be controlled by rotating a dial (not shown).

The schematic illustration of the spectrometer is shown in Fig. 1. The light is delivered to the spectrometer from the light source by an optical multimode fiber (core diameter 1 mm) and enters it through a variable entrance slit. The use of an optical fiber allows flexible coupling of light from various light sources into the spectrometer without the need of readjusting the spectrometer. The large fiber core enables straightforward delivery of light from relatively weak sources such as low-pressure gas discharge lamps or even indirect sunlight. The fiber core diameter was selected to illuminate the central third of the CCD camera. Consequently, a significant amount of the light delivered through the fiber is blocked by the slit (approximately 0.5% transmission). However, due to binning of the spectral line, the signal-to-noise ratio of the data is sufficient for the proposed experiments and light sources. Conversely, it is essential to take care to avoid saturation of the CCD camera, which could lead to distortions in the data. Nonetheless, for weaker sources, coupling efficiency can be enhanced by focusing the light exiting the fiber onto the slit, albeit at the cost of setup simplicity.

The slit is positioned at the focus of a 15° off-center parabolic mirror (focal length f=381 mm, diameter D=50 mm), which reflects the incoming divergent light into a collimated beam directed at an angle of $\beta=15^{\circ}$ to the mirror's axis. This collimated beam then illuminates the entire area of the reflection grating as required for maximum resolution. The ruled reflective diffraction grating has 300 lines per mm and 50×50 mm² area. Finally, the dispersed light is focused on the CCD camera by the second off-center parabolic mirror featuring the same $\beta=15^{\circ}$ and focal length f=381 mm, identical to the former one. The f-number of the imaging system is, therefore, f/#=f/D=7.6.

If the grating is at a rotation angle α , the central wavelength λ_c impinging on the detector is

$$m\lambda_c = 2d\sin\alpha\cos\beta,\tag{1}$$

where the integer number $m = \pm 1, \pm 2, ...$ represents the order of diffraction and $d = 3.3 \,\mu\text{m}$ is the line spacing of the grating. As such, one can precisely control λ_c by rotating the grating and thus changing α (see Appendix B for the derivation).

The detector is a commercially available color CMOS camera (model CS165CU, Thorlabs, Newton, NJ, USA). It features 1440×1080 pixels², each having $3.45 \,\mu \text{m}$ side length. The total active area is $4.968 \times 3.726 \,\mathrm{mm}^2$. Moreover, the camera is able to resolve colors. While this feature is not necessary in principle, it adds instructional value and has proven to be of great help for the students, as it simplifies the calibration process significantly. In particular, the students can more easily distinguish between the spectral lines that they use for calibration by their color. Furthermore, at the beginning of the experiment, when the students familiarize themselves with the functionality of the spectrometer, they can use the color information from the camera to distinguish between the zero and first order. For the zero-order configuration, the grating acts as a mirror and the spectrometer simply images the slit onto the camera. If the slit is illuminated by white light (e.g., by using the flashlight of their mobile phones), the image will be a white line. In this configuration, it is easy for the students to explore the imaging properties of the setup. By rotating the grating such that the first diffraction order is imaged onto the camera, the white light is dispersed by the grating, and a rainbow-like band of colors appears. Throughout their experiments, the students can use this technique to easily and quickly distinguish between the zero and first diffraction order.

The camera is connected to a computer via a USB connection, and the camera image is retrieved using the freely available ThorCam software, which can be downloaded from the Thorlabs website. This software enables users to capture live images from the camera and obtain (color-resolved) intensity information along both horizontal and vertical lines of pixels. The camera image can be exported as, for example, a bitmap file, which can then be imported into any data analysis software for further analysis (see Appendix D).

In order to operate the setup while it is enclosed in a protective box shielding it from room light, we prolonged the axis of the fine adjustment screw rotating the stage that holds the grating (see the inset in Fig. 2 and Appendix A). We added a turn dial that has an imprinted scale of 100 units per full rotation and that can count up to 10 full rotations. One unit of the scale k corresponds to a change of the angle of the grating of 58μ rad: $\Delta \alpha = \Delta k \cdot 5.8 \times 10^{-5}$ rad. Consequently, 10 full rotations ($\Delta k = 1000$) correspond to $\Delta \alpha = 3.3^{\circ}$. Within this range, we can approximate Eq. (1) for the first diffraction order as (see Appendix B)

$$\lambda_c \approx 2d \cos \beta (k - k_0) \cdot 5.8 \times 10^{-5} \approx (k - k_0) \cdot 0.37 \,\text{nm}.$$
 (2)

Here, k_0 corresponds to the position where the zeroth-order reflection from the grating is centered on the camera.

At this point, it is important to bear in mind that our spectrometer design is optimized for the undergraduate instructional laboratory. Better equipment (e.g., a more sensitive CCD, a piezo rotation stage instead of a manual rotation stage) would yield better results and make the setup even more powerful. However, we are convinced that the configuration presented here provides an optimal balance between cost, user-friendliness, availability, and pedagogical value.

A. Construction and functionality

1. Spatial and spectral resolution

The theoretical limit of the spectrometer's spectral resolution is given by its ability to image the light source (in our

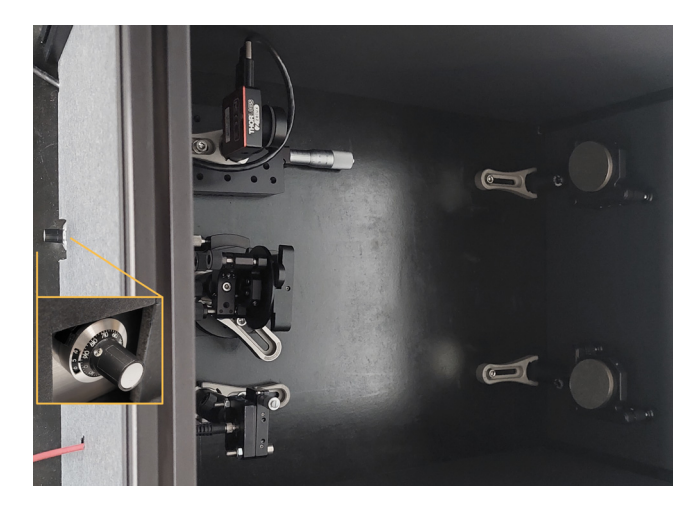


Fig. 2. (Color online) Photograph of the spectrometer. The top cover was removed for better visibility. The prolonged multiturn dial is shown enlarged on the left and described in more detail in Appendix A. The light is incoming from bottom left through a 1 mm diameter fiber (red) and follows the path indicated in Fig. 1.

case the illuminated slit) and the dispersion of the grating. Both of these properties are dependent on the focal length of the imaging setup. The Czerny–Turner layout of the spectrometer in a 4f configuration allows students to easily understand this interplay and is, therefore, particularly well-suited for a student lab experiment.

The spectrometer images the slit onto the camera. For an infinitesimally small slit, the standard deviation of the resulting Gaussian intensity distribution on the CCD camera is given in the paraxial approximation by

$$\sigma = \frac{2\lambda f}{\pi D} = \frac{2\lambda}{\pi} f / \#. \tag{3}$$

The full width at half maximum of the intensity distribution is then given by $FWHM = 2\sqrt{2 \ln 2} \sigma$. For a wavelength $\lambda = 500 \, \text{nm}$, we find $FWHM = 5.7 \, \mu \text{m}$. This is at the limit of what we can resolve with the pixel size of the camera of $3.45 \, \mu \text{m}$.

In reality, the imaging resolution is limited by aberrations⁴ and we find experimentally $FWHM_{\rm exp} \approx 13~\mu m$ (see Fig. 3). This value is a factor of 2.3 larger than expected, but it is sufficiently large such that the pixel size of the camera does not limit the resolution. Since the spectrometer images the slit 1:1 onto the CCD chip, the measured line width roughly corresponds to the slit size, which is significantly smaller than the accuracy of the micrometer screw used to adjust the slit size. In principle, a precision slit with a fixed width can be used to avoid this uncertainty, but we find that the adjustable slit is helpful to the students for both aligning the spectrometer and better understanding its functionality.

2. Spectral range of the spectrometer

The measuring range of the spectrometer is limited by the wavelength sensitivity of the CCD camera, which ranges from about 400 to 650 nm. The upper threshold comes from a factory-installed IR filter.

The rotation stage has a fine adjustment range of $\Delta \alpha = \pm 5^{\circ}$. This translates, according to Eq. (B2), to a range covering 1100 nm. For student labs, it is instructive to have

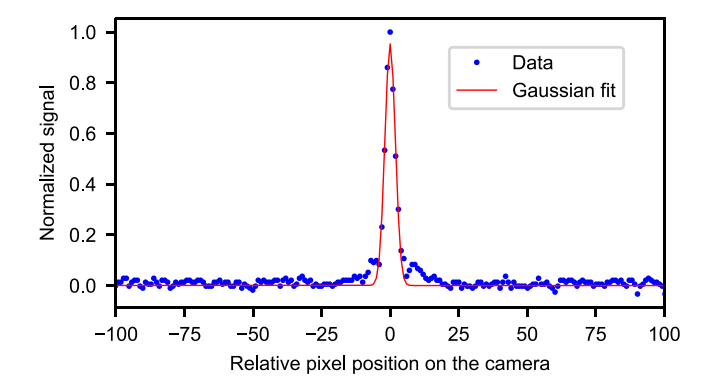


Fig. 3. (Color online) Line cut of the image of a slit with minimal width illuminated by a green LED. We plot the normalized signal in the green channel of the camera as a function of the relative position. The pixel number was converted to position from the image center using the pixel size of $3.45~\mu m$. The red line is a Gaussian fit to the data yielding a $FWHM_{exp}=12.9~\mu m$. In the inset, we show the resolution obtained from fitting an error function to the edge of the image of the slit as function of the slit width in μm .

the zeroth order visible on the CCD to help students understand the principle of the spectrometer. Using a white LED illustrates the difference between non-dispersive reflection (zeroth order) and dispersion (any other order) very well. In the present setup, the angle between zeroth and first order is about 4° .

For the linear dispersion, we obtain [see Eq. (B4) in Appendix B]

$$\frac{\Delta \lambda}{\Delta x} = \frac{d}{f} \cos \beta = \frac{3.3 \mu \,\text{m}}{381 \,\text{mm}} \cdot 0.9659 = 8.37 \,\text{nm/mm}.$$
 (4)

With this, we can calculate the spectral resolution of the spectrometer to be $\lambda_{spec}\approx 0.1$ nm, which is very comparable to other spectrometers based on off-the-shelf optics. The spectral width of a single image is limited by the size of the camera. We can cover a wavelength range of 42 nm over the 5 mm width of the CCD. Having a larger CCD chip would increase this range, but aberration effects would become significant. Already with the present chip dimension of 5 mm, we observe that the line width increases due to aberration by 10% toward the edge of the chip.

3. Reproducibility

So far, we have analyzed the spectral resolution limited by the optical properties of the spectrometer. Because the wavelength range covered by the CCD chip is much smaller than the full range of the spectrometer, it is essential that the rotation angle of the grating α can be precisely adjusted. In order to keep the setup simple and cost-effective, we use a manual stage to rotate the grating. The mechanical play and limited precision in reading the stage position then, of course, leads to systematic errors and finite settability of the grating angle.

We can read the stage position with a precision of $\Delta k = \pm 1$, which corresponds to a random error of $\Delta \lambda_c = \pm 0.37$ nm.

By performing repeated measurements of one spectral line when the turn dial is set to a certain position k, we can assess another systematic uncertainty: the reproducibility. We obtain an uncertainty of the central wavelength of 12 pixels. According to Eq. (B4), this corresponds to 0.3 nm, which is about 3 times larger than the spatial resolution. Combined with the precision in reading the turn dial position, which is ± 1 unit, we obtain a final resolution of $\Delta x = 83 \,\mu$ m or $\Delta \lambda = 0.65$ nm, respectively. This level of resolution is, of course, undesirable for a research-grade setup. However, we believe that it provides a good learning experience for the students. They can experience and explore the differences between statistical errors, which lead to the finite line width of the spectral lines, and systematic errors that manifest as deviations in the central position of spectral lines in repeated measurements.

III. APPLICATION IN STUDENT INSTRUCTIONAL LABS

A. Calibration of the spectrometer

Before using the spectrometer, we need to establish a relation between a wavelength of light $\lambda(p,k)$ that impinges on a given pixel p of the CCD camera for a given dial position k of the adjustment screw that controls the rotation of the diffraction grating. In order to do so, we calibrate the spectrometer using the bright spectral lines from the He lamp of known wavelengths, as are shown in Fig. 4(a). The calibration involves two separate steps. In the first step, we focus exclusively on finding the dependence of λ on k for $p = p_{\text{central}}$, corresponding to the center of the CCD. In the second step, we establish the dependence of λ on p for a

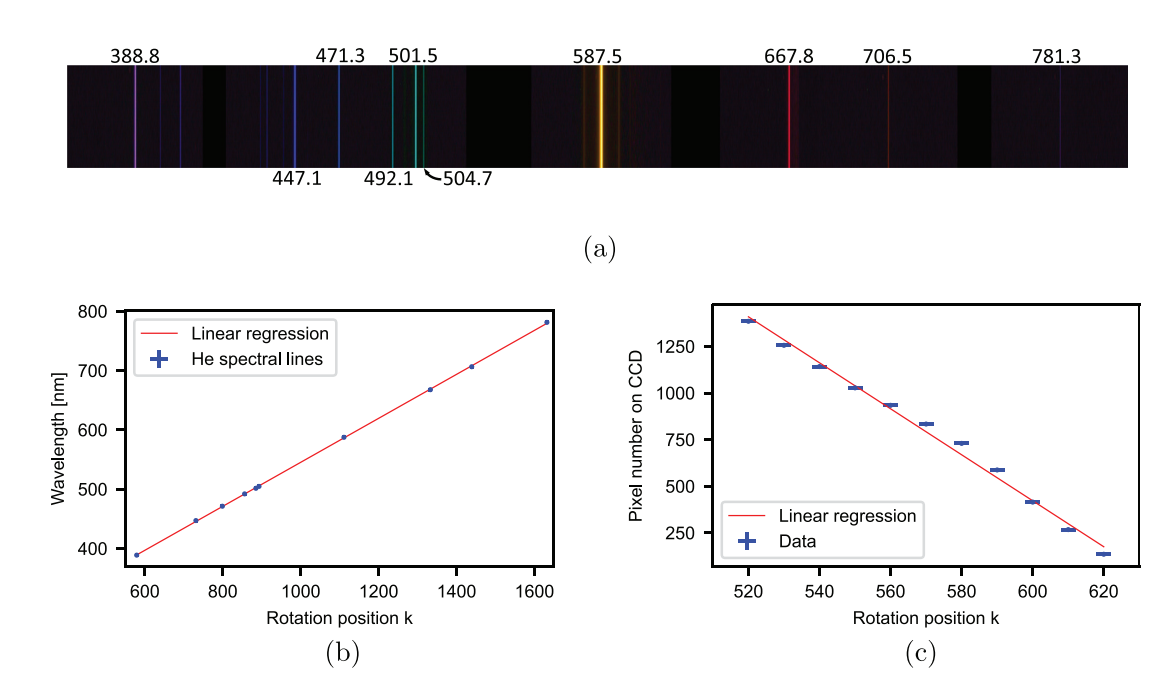


Fig. 4. (Color online) (a) Real images taken by the camera used for the calibration procedure, (b) calibration of the grating rotation angle, and (c) of the pixel column of the CCD camera. Both wavelength and pixel number on the CCD camera are expressed as function of the turn dial position k. (a) Collage of ten images of the He spectrum used for the calibration. Note that the position of the indicated wavelengths (Ref. 7), given in nanometer, are not to scale. (b) Wavelength on the central pixel column of the CCD as function of the angular position α of the grating. (c) Horizontal pixel number p onto which a fixed wavelengths impinges, as a function of different angular positions of the grating.

given k. These two steps are detailed in Subsections III A 1 and III A 2.

1. Calibration of the central wavelength

We start with calibrating the correspondence between the wavelength of light $\lambda_c(k) = \lambda(p_{\text{central}}, k)$ at the central pixel of the CCD camera and the dial position k. To achieve this, for each He spectral line, we adjust the grating angle to position this line at the center of the CCD (effectively operating the spectrometer as a monochromator). This allows us to determine the dependence of λ_c on k for all He lines, which is shown in Fig. 4(b). As expected from Eq. (2), the data points are very well described by a linear function of the form $\lambda_c = b(k - k_0)$ with k_0 and b being two fit parameters: $k_0 = -470 \pm 5$ and $b = 0.371 \pm 0.001$ nm. Note that at this point, it is instructive for students to validate the previously estimated wavelength uncertainty arising from the mechanical play of the adjustment screw, which can be calculated as $\Delta \lambda = b \Delta k \approx 0.4$ nm (taking into account that the precision of k readout $\Delta k = 1$).

2. Calibration of the wavelength-pixel relation

According to the derivation in Appendix B, the dependence of $\lambda(p,k)$ on p is expected to be linear with a slope that is independent of k. Bearing this in mind and considering the output of the first step of the calibration procedure, we can express $\lambda(p,k)$ in the following way:

$$\lambda(p,k) = b \cdot [(k - k_0) + (p - p_{\text{central}})/B]. \tag{5}$$

To determine the last unknown coefficient B, in the second calibration step, we select one He spectral line of a given wavelength and shift it across the CCD chip by tuning the dial position k. For each k, we acquire the CCD image and fit the line shape of the selected He line, allowing us to extract its pixel position p. The corresponding dependence of p on kis shown in Fig. 4(c). Similarly to the previous step, the data are well reproduced by the linear fit with $B = -12.3 \pm 0.5$. However, in this case, the overall quality of the fit is slightly lower, with the coefficient of determination yielding $r^2 = 0.993$ compared to $r^2 = 0.999914$ in Fig. 4(b). This difference is a direct consequence of the fact that the present data are obtained in a much narrower range of dial positions, which entails a larger influence of the mechanical uncertainty of the grating rotation. Consequently, relative uncertainties of k are visibly larger in Fig. 4(c). For this reason, the data points in this graph display larger deviations from the linear fit, although it still passes through>70% of points. This finally confirms the validity of the Eq. (5).

With the above-determined values of b, B, and k_0 , the spectrometer is fully calibrated and can be used for a wide variety of spectroscopic measurements. We will discuss three particularly valuable applications for student labs in Secs. III B-III D.

B. Spectrum of the sodium doublet

An illustrative example for students to experience the difference between statistical and systematic uncertainties can be found by investigating the sodium D-lines. In Fig. 5, we display the doublet, which can clearly be resolved. The wavelengths found in the literature⁷ for the D1 line is 589.59 nm and for the D2 line it is 589.00 nm. The measured

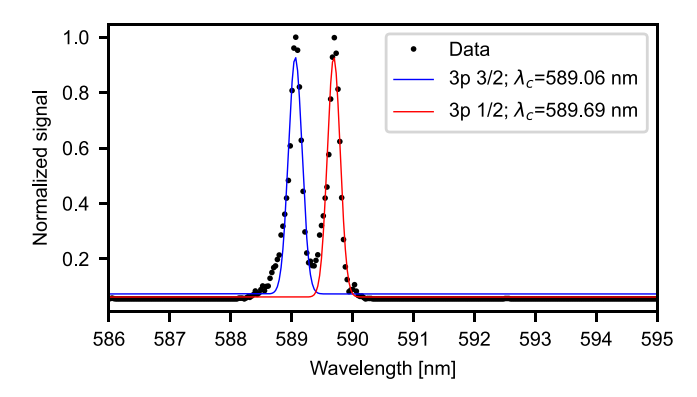


Fig. 5. (Color online) The spectrum shows the sodium doublet. The central wavelength λ_c of the two peaks is indicated in the figure. The relative separation between the peaks is $0.63 \,\mathrm{nm}$.

values we obtain are $\lambda_c = 589.06$ and $\lambda_c = 589.69$ nm, respectively, for the D1 and D2 line, in good agreement with the literature values.

C. Measuring the Balmer series

An instructive and historically important experiment is to measure the Balmer series of hydrogen. From this, the students can obtain a measured value for the Rydberg frequency $R_{\rm H}=R_{\infty}c$, where R_{∞} is the Rydberg constant and c is the speed of light. We show in Fig. 6 the composite spectrum of the Balmer series, consisting of four images taken with the camera. Using Eq. (5) allows us to calculate the wavelength of the Balmer lines. For comparison, the literature values are indicated as well. The uncertainty on the wavelength is the combined uncertainty from the central pixel p, i.e., σ_p , and the uncertainty on k, σ_k . The latter is identical for all four measurements, $0.4\,\mathrm{nm}$.

Note that the wavelength of the weak $H\delta$ -line cannot always be unambiguously determined with commercial gas discharge tubes. The noise level due to contamination is similar to the intensity of the spectral line, depending on the light source in use. Additionally, the sensitivity of the camera is low at these short wavelengths. Hence, we request the students to make a prediction about the wavelength of the $H\delta$ -line by calculating the Rydberg frequency according to the well-known equation

$$\nu = R_{\rm H} \left(\frac{1}{m^2} - \frac{1}{n^2} \right),\tag{6}$$

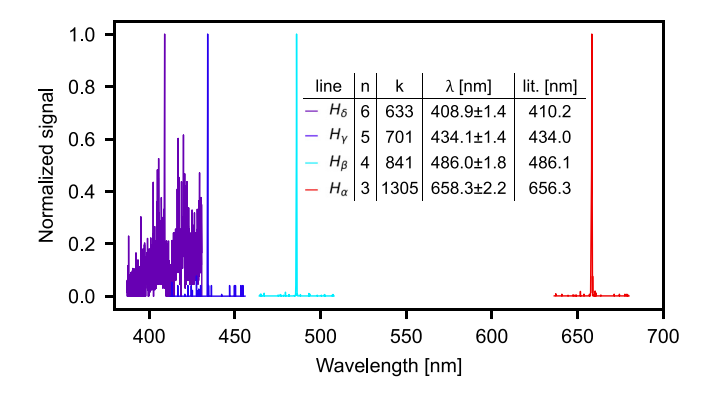


Fig. 6. (Color online) Spectral emission lines of an H_2 spectral lamp, as function of the wavelength λ . The central wavelength indicated in the figure is determined from a Gaussian fit.

where m=2 denotes the Balmer series, n=3, 4, 5, and corresponds to the Balmer lines $H\alpha$, $H\beta$, $H\gamma$, and $H\delta$, respectively, and $\nu=c/\lambda$ is the frequency of the corresponding line. The Rydberg frequency obtained from the data, $R_{\rm H}^{\rm data}=(3.28\pm0.01)\times10^{15}\,{\rm Hz},$ is in good agreement with the literature value of $R_{\rm H}=3.29\times10^{15}\,{\rm Hz}$. Hence, from the above equation, we obtain an estimate for the wavelength of $H\delta$: $\lambda_{\rm H\delta}\approx408$ nm. This allows fitting the hydrogen spectrum with well-constrained initial parameters, and $\lambda_{\rm H\delta}$ is found to be $408.9\,{\rm nm}$.

D. Observation of Fraunhofer lines

Another interesting task for students is observing the Fraunhofer absorption lines in the solar spectrum. Because we use an optical fiber to guide the light toward the collimator slit, it is simple to hold the fiber end toward the sunlight. In this way, we can ensure sufficient sunlight is being coupled into the spectrometer, while the CCD camera remains shielded from stray light. The CCD camera is sensitive enough that no direct illumination of the fiber facet is necessary, but a cloudy sky is sufficient. We show in Fig. 7 an excerpt of the solar spectrum, spanning over 40 nm. In this particular spectrum, we find the H_{β} -line of hydrogen, as hydrogen is a constituent of the Sun. An additional four Fraunhofer lines were found, and two could be identified. Of course, there are many more features in the shown spectrum, such as the natural decrease in signal strength toward low wavelengths. The solar spectrum offers rich physics, and it is up to the instructors of a lab course to select suitable tasks for students.

IV. CONCLUSION

In conclusion, we present and characterize a cost-effective Czerny–Turner optical spectrometer for physics student lab experiments. The setup is assembled from standard optical and mechanical components with very little additional machining required. Despite the compromises that have to be made regarding optical and spectral resolution, as compared to research-grade laboratory equipment, the presented setup allows for remarkably high-resolution spectroscopic measurements for a student lab. The resolution of the proposed spectrometer was optimized simultaneously for high performance, pedagogical value, and simplicity in operation and understanding of spectrometers. The working principle of the spectrometer is straightforward and it can easily be

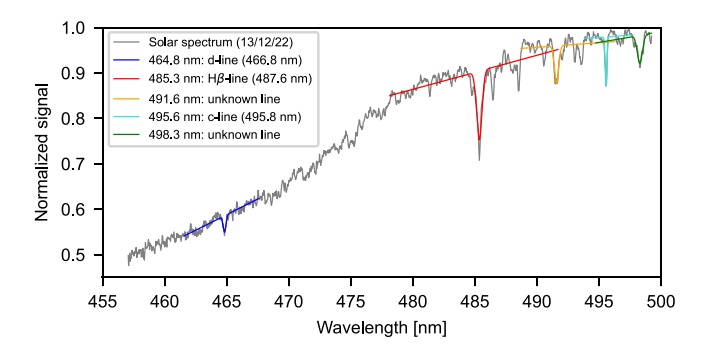


Fig. 7. (Color online) Solar spectrum between 455 and 500 nm. Included are the fits to the H_{β} -line and four other Fraunhofer absorption lines. The central wavelengths were obtained from fitting a Gaussian to the data and can be compared to literature values (Ref. 11).

understood and operated by undergraduate physics students, particularly as compared to more traditional telescope-based setups usually used in student labs. Because of its simple setup and transparent working principle, the students are able to get a full understanding of a spectrometer, and, if desired, they can set up the spectrometer themselves. Moreover, the use of a (color) CCD camera not only simplifies the operation and helps build intuitive understanding for students, but it also allows for quantitative data acquisition. The subsequent computer-based data analysis, including fitting and plotting of the data, provides the students with a good insight into modern experimental physics.

We have discussed two hallmark experiments that can be performed in an undergraduate physics lab course: measurement of the Balmer series and the observation of Fraunhofer lines. Further experiments that can be readily performed with the use of this spectrometer include the investigation and determination of unknown light sources. Here, the use of an optical fiber is of particular advantage: even spectroscopic analyses of flames are possible.

ACKNOWLEDGMENTS

The authors gratefully acknowledge Li Bing Tan, who helped in testing the setup and greatly improved the student manual.

AUTHORS DECLARATIONS Conflict of Interest

The authors have no conflicts to disclose.

APPENDIX A: PROLONGED TURN DIAL

Figure 8 shows the prolonged turn dial which controls the angular position of the grating. The rotation stage (model XRR1, Thorlabs, Newton, NJ, USA) has a knurled screw head on a fine thread to turn it. Because the knurled screw head moves in and out while turning it, we added a hex key that could slide in and out the white tube. This allowed us to compensate for the longitudinal movement, and hence, the turn dial could be mounted in a fixed position. On the turn dial, there is an imprinted scale ranging from 0 to 100, which helps to read the position of the grating.

APPENDIX B: DERIVATION OF EQUATIONS

Generally, for a plane wave incident at any arbitrary angle $\varphi_{\rm in}$ to the grating normal, and with an outgoing angle $\varphi_{\rm out}$ relative to the grating normal, we obtain for a grating with grating constant d the central wavelength λ_c of the mth-diffraction order (see Ref. 10)

$$m\lambda_c = d[\sin(\varphi_{\rm in}) - \sin(\varphi_{\rm out})].$$
 (B1)

In our case, where the grating is at a rotation angle α , we obtain λ_c as

$$m\lambda_c = d[\sin(\beta + \alpha) - \sin(\beta - \alpha)] = 2d\sin\alpha\cos\beta,$$
 (B2)

where β corresponds to the off-centricity of the mirrors, and the integer number $m=\pm 1,\pm 2,\ldots$ represents the order of diffraction. As such, one can precisely control λ_c by rotating

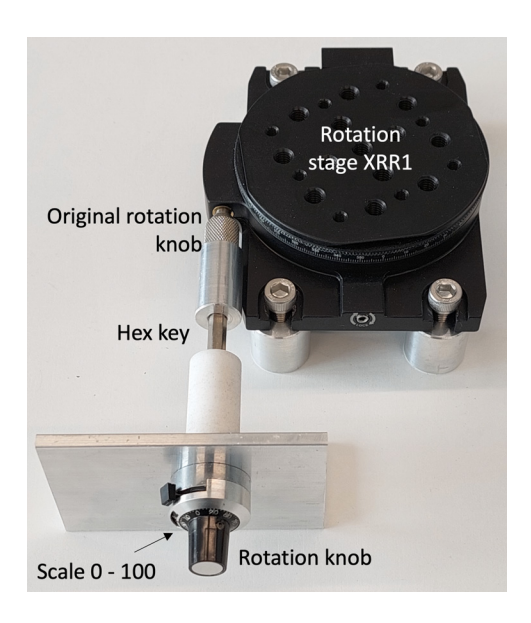


Fig. 8. The rotation stage (model XRR1, Thorlabs, Newton, NJ, USA) was modified by adding a turn dial with an imprinted scale from 0 to 100. Using a hex key which could slide along its axis compensated for the longitudinal movement of the original turn dial along the fine thread.

the grating with the use of the attached dial thus changing α . In addition, the CCD camera sensor has a certain size: it contains of an array of 1440×1080 pixels (horizontal \times vertical), each of which being a square with a side length of $s_p = 3.45 \, \mu \text{m}$. The light focused on pixels separated horizontally by a given distance of Δx is diffracted by the grating at a slightly different angle differing by $\Delta \alpha = \Delta x/f$. This means that two rays differing by $\Delta \lambda$ can be related to $\Delta \alpha$ using the formula describing the diffraction maxima for the reflective grating:

$$m(\lambda_c + \Delta \lambda) = d[\sin(\beta + \alpha) - \sin(\beta + \Delta \alpha - \alpha)]$$

$$\approx 2d \sin \alpha \cos \beta - d\Delta \alpha \cos(\beta + \alpha), \quad (B3)$$

where we assumed that $\sin(\Delta\alpha)\approx\Delta\alpha$ and $\cos\Delta\alpha\approx 1$ (which is justified for small $\Delta\alpha$; in our case, $\Delta\alpha\approx 5$ mm/381 mm = 0.013 over the full range of the CCD). Combining this equation with the previous one, we get

$$m\Delta\lambda \approx -d\Delta\alpha\cos(\beta + \alpha) = -\Delta x \cdot (d/f)\cos(\beta + \alpha)$$

$$\approx -\Delta x \cdot (d/f)\cos\beta,$$
 (B4)

where we assumed that α is small. This relation implies that the light focused on subsequent horizontal pixels of the CCD camera has a different wavelength changing linearly with the position across the CCD sensor. As such, by taking an image of the CCD camera, we can measure the spectrum of light within the wavelength range $\Delta \lambda = (s_C/m) \cdot (d/f) \cos \beta$ (defined by the size s_C of the CCD sensor and the diffraction order m) around the central wavelength λ_c controlled by the grating angle α [as described by Eq. (B2)]. By changing this angle, one can thus acquire spectra in any wavelength range.

APPENDIX C: LIST AND DESCRIPTION OF PARTS

We list in Table I the components used to assemble the spectrometer. The prices are given for the total number of pieces and reflect the prices in early 2023. The total price including one spectral lamp is given as well. Our students bring their own computer; hence, these cost are not considered. In order to reduce the cost, an individual base plate such as a wooden board (e.g., MDF, 25 mm thick and 600×450 mm side length) can be used, where one drills holes and uses thread screw inserts. This saves about $350 \in$.

Table I. List of the components used to assemble the spectrometer.

Qty	Part number	Description	Distributor	Price (€)
2	MPD2151-P01	15° Off-Axis Parabolic Mirror	Thorlabs	735
1	GR50-0310	Reflective Diffraction Grating 300/mm	Thorlabs	200
2	KS2	2"Mirror Mount	Thorlabs	277
1	SM1T10	Adapter for Camera	Thorlabs	21
1	SM1A11	Adapter for Camera	Thorlabs	21
1	KGM60	Kinematic Grating Mount Adapter	Thorlabs	173
1	PH40E/M	Pedestal Post Holder $L = 44.7 \text{ mm}$	Thorlabs	25
4	PH100E/M	Pedestal Post Holder $L = 104.7 \text{mm}$	Thorlabs	106
1	TR40/M	Optical Post $L = 40 \text{ mm}$	Thorlabs	5
4	TR75/M	Optical Post $L = 75 \text{ mm}$	Thorlabs	22
1	XRR1/M	Rotation Stage	Thorlabs	428
1	CF125C/M	Clamping Fork 31.5 mm	Thorlabs	11
4	CF175C/M	Clamping Fork 44.4 mm	Thorlabs	50
1	VA100/M	Adjustable Mechanical Slit	Thorlabs	268
1	CS165CU/M	Zelux _® 1.6 MP Color CMOS Camera	Thorlabs	428
1	XR25C/M	Linear Translation Stage	Thorlabs	448
1	MB4560/M	Breadboard (Baseplate) 450 × 600 mm	Thorlabs	390
1	M35L01	Multimode Fiber $1000 \mu \text{m}$, 0.39NA	Thorlabs	99
1		Elongated Turn Dial (self-made)	Workshop	10
		Optional: Light protective box		
4	XE25L300/M	Construction Rail 300 mm	Thorlabs	68
2	XE25L375/M	Construction Rail 375 mm	Thorlabs	41
2	XE25L525/M	Construction Rail 525 mm	Thorlabs	54

TABLE 1. (Continued)

Qty	Part number	Description	Distributor	Price (€)
4	RM1S	1" Construction Cube	Thorlabs	82
1	SH6M8LP	M6 × 1.0 Channel Screw (50 Pack)	Thorlabs	16
5	•••	Black cardboard sheets 4 mm	Office Store	15
1	e.g., 1 045 162	Spectral lamp (e.g. He, H ₂ ,)	Conatex	70
	•••	Total cost for 1 setup	•••	4063

APPENDIX D: SOFTWARE TO ANALYZE THE DATA

In the following, the main steps to analyze the data are given. For the analysis, we recommended to use Python as analysis software since our students are familiar with it, but there are many alternatives, and the steps outlined below are valid for any programming language.

- Read in the bitmap file created from the ThorCam software into the analysis program. In python, one option is to use "image" from the "PIL"-package, allowing to use the simple command "plot.imread(filename)."
- The image can now be processed within python. For our purposes, it is sufficient to create a matrix with the *x* and *y*-coordinates and the intensity level for all three colors.
- For a basic analysis, as applied here, it is sufficient to add all the three color intensity values, resulting in a twodimensional array with the integral intensity value per pixel.
- In order to increase the signal-to-noise ratio, we suggest to our students to take a line cut consisting of about 20–50 vertically averaged pixels, typically from a central region of interest. This results in a sufficiently smooth horizontal line cut, as shown in Fig. 3. Note: Depending on the tasks, students are asked to investigate the signal-to-noise ratio in more detail.
- The line cut can now be investigated according to the task at hand. For most applications it is sufficient to use a Gaussian function to fit the spectral lines in order to obtain the mean of the Gaussian and its width.

- In order to fit the solar spectrum (as in Fig. 7), it is favorable to invert the spectrum (multiply with -1) and fit the inverted spectrum. Care has to be taken when choosing the starting values and fit range, in order to ensure good convergence of the fit.
- a) Author to whom correspondence should be addressed: egandrea@phys. ethz.ch, ORCID: 0009-0002-7958-3239.
- b)ORCID: 0000-0001-8154-5990.
- ¹Compact CCD Spectrometers, see https://www.thorlabs.com/ for "CCS100."
- ²Alexander Scheeline, "How to design a spectrometer," Appl. Spectrosc. **71**(10), 2237–2252 (2017).
- ³M. Czerny and A. F. Turner, "Über den astigmatismus bei spiegelspektrometern," Z. Phys. **61**(11–12), 792–797 (1930).
- ⁴M. A. Gil and J. M. Simon, "New plane grating monochromator with off-axis parabolical mirrors," Appl. Opt. 22(1), 152–158 (1983).
- ⁵R. A. Hill, "Rapid scan spectrometers for the diagnostics of transient plasmas," Appl. Opt. 7(11), 2184–2189 (1968)).
- ⁶Q. Yuan, D. Zhu, Y. Chen, Z. Guo, C. Zuo, and Z. Gao, "Comparative assessment of astigmatism-corrected Czerny-Turner imaging spectrometer using off-the-shelf optics," Opt. Commun. 388, 53–61 (2017).
- ⁷See https://physics.nist.gov/PhysRefData/ASD/lines_form.html for "the atomic spectral data about the sodium lines."
- ⁸A. Kramida, Yu. Ralchenko, J. Reader, and NIST ASD Team, *NIST Atomic Spectra Database (Ver. 5.10)* (National Institute of Standards and Technology, Gaithersburg, MD, 2022).
- ⁹E. Tiesinga, P. J. Mohr, D. B. Newell, and B. N. Taylor, "CODATA recommended values of the fundamental physical constants: 2018," J. Phys. Chem. Ref. Data **50**(3), 033105 (2021), Table XXX.
- ¹⁰D. Halliday, R. Resnick, and J. Walker, *Fundamentals of Physics*, 10th ed. (Wiley, New York, 2013).
- ¹¹J. Mitton, "The stronger absorption lines in the solar spectrum an identification list," J. Br. Astron. Assoc. 85, 238–241 (1975), https://ui.adsabs.harvard.edu/abs/1975JBAA...85..238M.